New Dimensions for Solar Evaporation Site Analysis

H. L. Bradley and R. F. Langill
Salt Consultants and Engineers, Newberry, Florida, USA
and
Richard F. Langill & Associates, Inc., Germantown, Maryland, USA

ABSTRACT

The availability of Landsat imagery adds a new dimension to selecting and evaluating solar evaporation sites. Landsat imagery is particularly useful early in a project when conventional maps and air photos are not available. This paper presents information on imagery interpretation and its application to locating suitable areas for siting solar evaporation ponds. Remote sensing images at available scales provide a rapid and inexpensive dimension or tool for screening large areas and selecting sites with potentially favorable geohydrological conditions. Processed multi-spectral and single band imagery provide additional data for evaluating specific solar evaporation pond site characteristics to assist in design and engineering.

Satellite imagery was applied to evaluating geology and hydrology at a number of locations, including three sites in Venezuela where storm tides and excessive surface water run-off posed a potential problem. Expansion of solar ponds and crystallizers was completed at one of the locations after solving many unique problems. A Phase 1 expansion has been completed at the second site, and the third remains under investigation.

An extensive study of technical reports on solar evaporation was made in connection with the Venezuelan site evaluations. This paper presents a number of invaluable graphs, charts, nomographs and formulae compiled during the study and applies these data to solar evaporation pond design, construction and operational procedures.

INTRODUCTION

Satellite imagery is an invaluable tool to select and evaluate sites for solar salt production. Large-scale images covering thousands of square miles can be reviewed in a matter of minutes to select and compare sites for further study. Magnified and processed images in black and white and false color provide more detailed data on site conditions for evaluating the feasibility of pond construction at selected locations.

Solar evaporation pond site selection is usually carried out on a regional or country-wide basis to determine the location of suitable land areas in proximity to transportation and shipping facilities. After initial site selection, evaluations are directed to obtaining detailed data on geological and hydrological factors affecting pond design and engineering.

IMAGE PROCESSING

Images obtained by Landsat remote sensing are extremely useful for both studies. The unprocessed image area for a single frame covers about 13,000 square miles. An image is obtainable in usable form for site selection procedures with a scale of about 1:250,000. The image can be rapidly scanned to locate sizeable areas with tonal variations signifying flat ground or low-lying swampy areas potentially suitable for solar pond construction. Landsat sensors obtain images in four or more separate bands or wave lengths. Site screening and selection studies can be based on tonal variations for a single band that provides indications of soil moisture and surrounding terrain characteristics. A Band 5 image generally gives the best display of geological features, soil moisture, and the location of the land-water interface (Figure 1).

Bands 4, 5 and 7 are composited to yield an image in false color for detailed site evaluation prior to field studies. The variations in color and tone on the image show the health and distribution of vegetation, moisture content of the soil, depth of water adjacent to the area and site geomorphology. It is often helpful to enlarge or magnify the image by photographic processing to a scale of either 1:20,000 or 1:50,000 for detailed site evaluations. Single bands can be used jointly or separately with multi-spectral false color to provide data on soil moisture and geomorphology. We have found the combination of Bands 4, 5 and 7 provides usable data at the least cost for both site selection and evaluation.

The enlarged imagery scales recommended for site evaluation studies are commonly used as a base for topo-

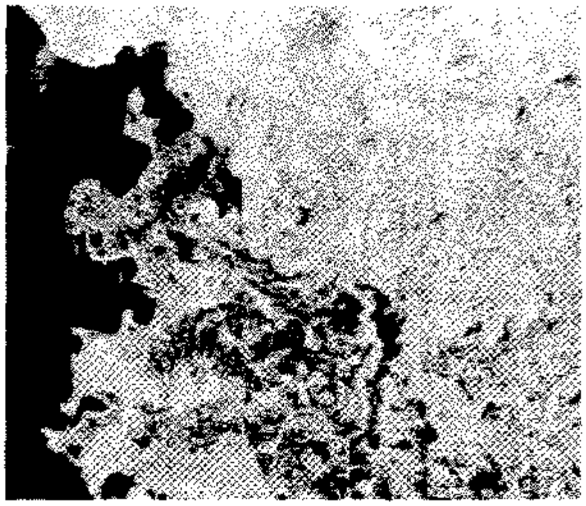

Figure 1. Band 5 black and white of area near Ganaine, Haiti. The north-south distance is approximately 22 miles.

graphic mapping. If topographic maps are available for a selected site, a clear overlay of the map should be prepared to match the scale of the image enlargement. When field investigations are implemented, features on the image can be directly referred to topographic map features and elevations. It may also be helpful to obtain images for a particular site during the wet and dry season. Our efforts to obtain useful seasonal data have been unsuccessful, either because of local or seasonal cloud cover in the area of interest or the satellite image sensors were turned off.

SENSOR DESCRIPTION AND COMPARISONS

As previously noted, Landsat images are available in four separate bands. The four bands designated 4, 5, 6 and 7 occur in two visible and two invisible portions of the spectrum, ranging from green through red to near infrared. The various sensing bands and their wavelengths are as follows for Landsat 1 through 3:

Band Number	Wavelength in Micrometers
4	0.5 to 0.6 visible—green
5	0.6 to 0.7 visible—red
6	0.7 to 0.8 invisible—near infrared
7	0.8 to 1.1 invisible—near infrared.

Sub-scene images of each individual wavelength from a Landsat Multispectral Scanner (MSS) ranges in tonal variation from white through grey to black, depending upon the wavelength reflected from the object. As stated succinctly in Petroleum Engineer International, "these images are invaluable to the geologist because of their synoptic aspects—a single scene surveys a wide variety of terrain, geology and landform types under near optimum viewing conditions that enhance or emphasize the relationships of surface features." (Sept. 1980, p. 146) Vegetation shows up best in the near infrared and water is best indicated in the green band. On false color composites, using Bands 4, 5 and 7, healthy vegetation appears in red and clear deep water in black. In a sparsely covered area typically selected for additional study, false color variations, appearing as red, green and black, are used to identify or infer geological and hydrological features impacting on pond construction and operation. Interpretations of favorable and unfavorable siting characteristics are all subject to field confirmation.

The possible use of Landsat imagery for interpreting technical and environmental solar evaporation siting factors are shown below in Table 1. This table is adapted from a publication by David J. Barr (1972).

APPLICATION TO SITE INTERPRETATION

Landsat imagery was used for siting studies in a number of countries with varying terrains. As one example, we were assigned to locate a suitable site for solar ponds near a proposed petrochemical complex on the Arabian Gulf in Saudi Arabia. Standard aerial photography was not available because of government regulations. A Landsat image was readily available in Band 5 and we were able to identify three flat sabkha or swamp areas about 15 miles from the proposed complex. The satellite image was taken during the wet season, so we were reasonably assured the areas were not normally subject to flooding by Arabian Gulf storm tides or seasonal surface water dis-

TABLE 1

Siting Factors and Sensor Use

SITING FACTOR	IMAGERY SATELLITE
Topography	I-F
Site Size	M
Existing Land Use	D
Existing Bodies of Water	D
Extent of Vegetative Cover	D
Diseased (affected) Vegetation	I-F
Regional Geology	I-F
Local Geology and Soils	I-F
Local Erosion	I-F
Deposition-Siltation	I-F
Soil Moisture Condition	I-F
Regional Hydrology	I
Local Hydrology	I-F
Pollutional Discharges	I
Lagoon Leaks	I-F
Discharge Dispersion	I-F
Flooding Potential	I-F

Key: M = Measure
I = Infer with high confidence
I-F = Infer subject to field check
D = Detect

charge. One of the areas selected for soil borings and permeability tests had variations similar to the tonal signature at two saline deposits about 60 miles away. The available literature indicated that this salt deposit was both limited in size and thin. Field investigations confirmed the image interpretation, revealing a large 20-square-mile salt deposit. Later drilling showed the mineable salt thickness exceeded 25 feet. At the other two Saudi Arabian sites, testing showed permeability coefficients ranging from poor to fair and a recommendation was tendered to exploit the sabkha salt deposit.

Two later assignments involved selection and evaluation of sites in Haiti and the Dominican Republic. A number of Band 5 images for coastal areas in both countries were obtained and examined. Some of the preferred locations were too small to provide the requisite salt tonnage. Other areas had excessive water depths behind barrier beaches with drainage patterns indicating high surface water run-off. Three sites were selected for further investigation and magnified false color images were obtained for detailed studies. Inspection of false color image of the three sites selected for detailed evaluation revealed an extensive drainage system that was not apparent on the Band 5 image or topographic map. Through a subsequent inquiry, we found that an agricultural land reclamation program would eventually incorporate part of the area needed for solar ponds. This consideration nullified the need for additional evaluations.

Standard aerial photography and topographic maps were available for the remaining two sites. At the only Haitian site, imagery studies confirmed with a field check indicated a potential for inundation of proposed concentration and crystallizer pond locations from storm tides and the possibility of breaching the landward side of the crystallizer dikes from flash flooding due to seasonal precipitation in the mountainous interior.

Problems at the third site located in the Dominican Republic differed significantly. Comparison of the Landsat imagery and air photos with available geologic maps showed that the mapped boundary of a water-bearing karstic limestone was not correctly located. After adjustment of the land area, the facility was reduced by about 40 percent. A further interpretation of vegetation patterns and tonal variations suggestive of soil moisture indicated the karstic limestone dipped gently seaward below the site with ground water rising near the surface through the overlying soil and rock. This local hydrologic condition was confirmed by field observations of underwater springs offshore and seeps and springs along the beach bordering one side of the site.

In summary, the use of satellite imagery adds a new dimension for locating sites for solar evaporation ponds. Imagery has been successfully used as a tool for site selection and evaluation to determine competing land use, the extent of vegetative cover, regional and local geohydrologic conditions, local geomorphology and other factors of interest to solar pond design and engineering.

Use of a positive Landsat image in a single band is recommended in selecting sites for further evaluation. Use of a false color image generated by compositing three or four bands is an acceptable alternative, especially when geologic and topographic maps are not available.

It is usually necessary to expand the scale of an image to conduct a further evaluation of a selected site for design and engineering. The expanded or processed image should match the scale of available cartography. Many factors affecting solar pond construction can be inferred from the expanded image prior to visiting the site. We recommend confirming all inferences obtained through image interpretation by field inspection at the prospective site.

PROCEDURE FOR DETERMINING SOLAR SALT MAKING CAPABILITY OF A SITE

Before this procedure was prepared to evaluate sites in Venezuela an extensive review was made of technical reports on the art and science of solar salt making and solar evaporation. Procedures were devised to evaluate the factors affecting the productive capability of a site. For the sake of brevity, recognition of the many contributions by these authors is restricted to the annexed bibliography. The principal precaution offered is to be wary, as no two salina sites have completely comparable conditions.

Weather Station Data

Procedures are well established and documented for recording pertinent weather data. Good judgment is required when extrapolating historical data from a weather station to apply to a prospective solar salt site. The weather can vary drastically within a few miles and the author has observed serious mistakes made in attempting to extrapolate data from one area to another.

Evaporation

The starting point for determining salt production begins with the measurement of fresh water that evaporates per 24-hour period measured in millimeters from a 48-inch diameter, 10-inch-high galvanized pan placed on 2″×4″ supports at ground level called a standard U.S. Class A evaporation pan. There are also other standard pans.

In most cases evaporation data for a site being evaluated does not exist. Until a weather station can be provided and at least a year of recordings made, an approximation can be calculated from wind speed by use of one of several formulas. A plot of the findings of six different authors of evaporation per day, versus wind speed in M/sec was assembled by Salin du Midi. From the writers' experience the Penman B formula $E = 0.14\ (1 + 0.88V)D$, or Sutton's formula, correlates pond evaporation of fresh water and wind speed. Wind records more frequently are available than evaporation records, i.e., airports, large farming operations. At Araya, Venezuela, for example, the wind speed had been recorded by Salina personnel at 33.7 Km/hr, while at another location several miles away at 22.3 Km/hr. At 33.7 Km/hr wind velocity there would be an evaporation of fresh water of over 5.0 M/yr which was obviously in error. The location having 22.3 Km/hr checked out with fresh water pan evaporation records of 3.391 M/yr.

Penman confirmed that in areas having wind movement in excess of 1.34 M/S, fresh water lake evaporation was approximately equal to fresh water pan evaporation. Below 1.34 M/S an appreciably lower ratio existed between ponds and evaporation pans.

Evaporation Factor

The evaporation factor is necessary to establish for a site the ratio of the evaporation of brine to fresh water and is greatly affected by the vapour pressure (which in turn is influenced by Mg^{++} content of the brine); therefore, the higher the salinity (Mg^{++} content) the lower the evaporation factor (Figure 2).

Salins du Midi published data that the company had gathered to demonstrate the relationship between temperature of fresh water, relative humidity and of vapour pressure of brine (v.p. of fresh water vs temperature is known) and presented a formula for calculating the evaporation factor using a derivation of Sutton's formula. These data have been plotted into a nomograph for ease of use and accuracy by Dale Krrmse Ph.D., P.E., University of Florida (Figure 3).

Relative Humidity

Relative humidity data taken over a one-year period provided fairly reliable data but should be recorded on a 24-hour basis. Such data very seldom exists at a new site; however, there may be readings taken at a nearby airport at 7 A.M., 1 P.M. and 3 P.M. The daily mean R.H., from the authors' experience, will approximate the average of the 7 A.M. and 1 P.M. readings. The 3 P.M. reading should be discarded in determining the mean. This can be verified for a site by using a recording R.H. Meter over a period of several weeks. Caution is needed in using published R.H. data, since the observer may not have realized the importance of taking R.H. at the specified time of day and in his accuracy of measurements. The mean R.H., given at 3-hour intervals around the clock, and the average of the 7 A.M. and 1 P.M. readings, at Palisadoes Airport, Kingston, Jamaica was 74% between 1955 and 1971 and the average of the 7 A.M. and 1 P.M. readings was 73%, which is reasonable agreement.

By use of the nomograph the evaporation factor for Araya, using 28°C fresh water evaporating pan temperature, R.H. of 76% and average brine Be′ of 28 (25 g/1 Mg^{++}), is read at 0.57 of brine in crystallizers or $3.391 \times 0.57 = 1.93$ meters evaporation.

Rainfall

Excessive rainfall makes solar salt production impractical in many sites. In calculating the net evaporation it must be remembered that rainfall evaporates at a rate equal to brine, i.e., (gross evap. × evap. factor) minus rainfall = net evaporation. Errors have been made at times by deducting rainfall from gross evaporation and then multiplying by the evaporation factor, i.e., (gross evap. minus rainfall) × evaporation factor. This calculates to an erroneously high net brine evaporation.

Careful study of rainfall patterns for the site is essential, i.e.,

1. Average monthly rainfall
2. Maximum one-day and two-day rainfall per month
3. Variations in rainfall per month
4. Determine if there is a pattern of wind direction and velocity during and after rainfall, (evaluate suitability of using automatic floating decants in crystallizers and saturated brine ponds to remove top surface weak brine
5. Determine best months to harvest
6. Evaluate chances for catastrophic rainfall reducing or eliminating salt harvest.

At Araya, Venezuela net evaporation becomes $(3.391 \text{ M} \times 0.57) - 0.188$ M rainfall = 1.742 M. Then deduct for time the crystallizer will be drained, harvested and refilled $(1.742 \times 350/365 = 1.671)$.

BRINE RECOVERY IN CRYSTALLIZER

Salt recovery from original feed brine to crystallizer is illustrated in Figure 4. When dumping brine from crystallizers at 29.0 Be′ (bittern), 76% of the NaCl is recovered (Figure 4). Saturated brine contains 271 g/l NaCl, so that if 76% of the salt in brine is recovered, 206 g/l is deposited. Salt deposited then becomes 3,442 M ton/ha [$10{,}000 \text{ M}^2 \times 1.671 \text{ M} \times 206 \times 10^3/10^6$] (Figure 1).

At this point losses in harvesting, washing, stockpile shrinkage and scale losses are then applied to arrive at the salt saleable. But this is another subject.

SERIES OPERATION

Tests have been recorded indicating that 10% more salt is produced in crystallizers by operating crystallizers in series of 3 or 4 ponds to maintain a lower average 27.6 Be′ brine (lower Mg^{++}), compared to operating in parallel of 28.2 Be′. By use of nomograph the evaporation factor would be reduced from 0.57 to 0.48 or 16% less (Figure 3).

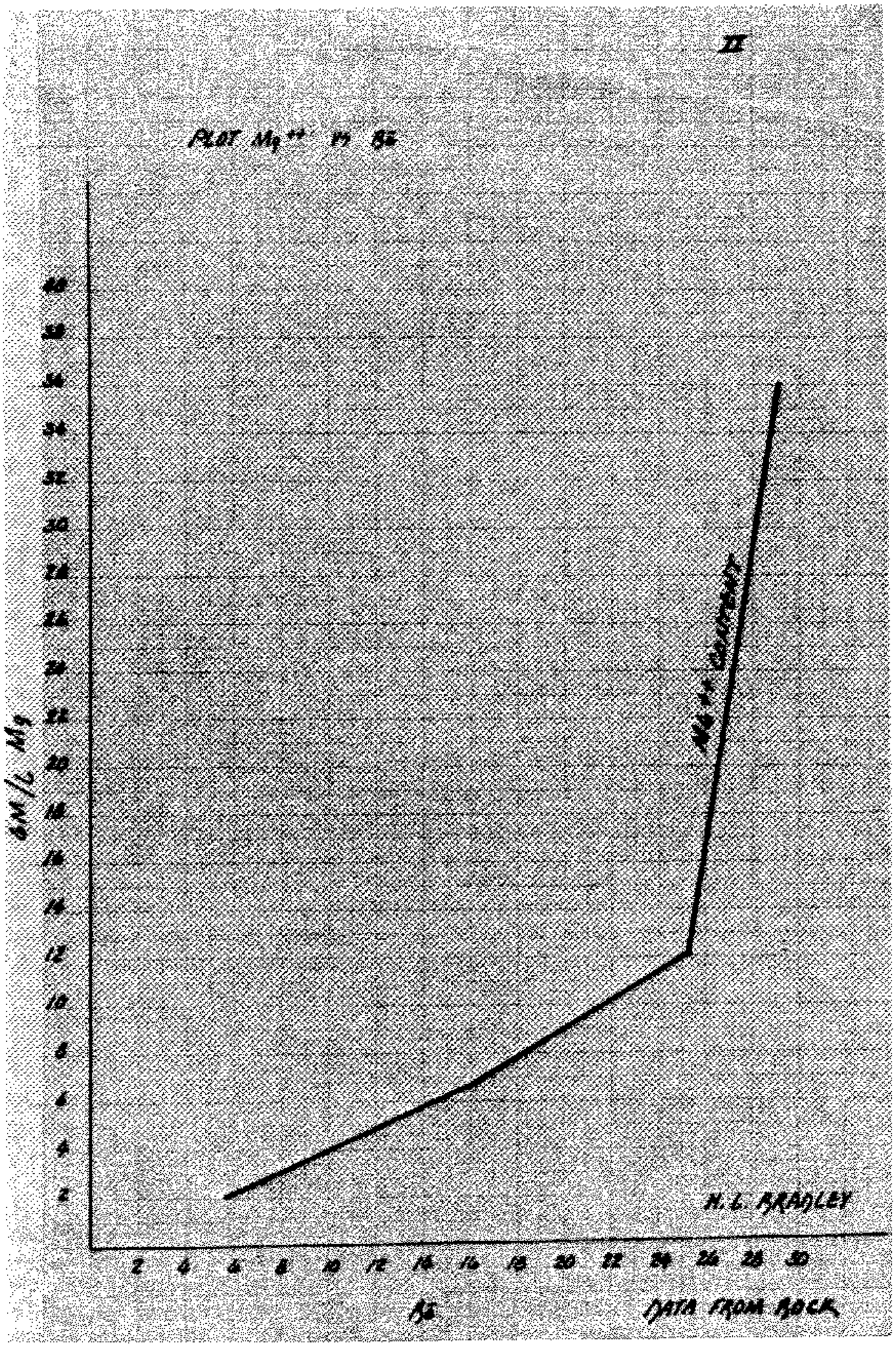

Figure 2. Graph Mg^{++} vs Be′ (Data from Bock)

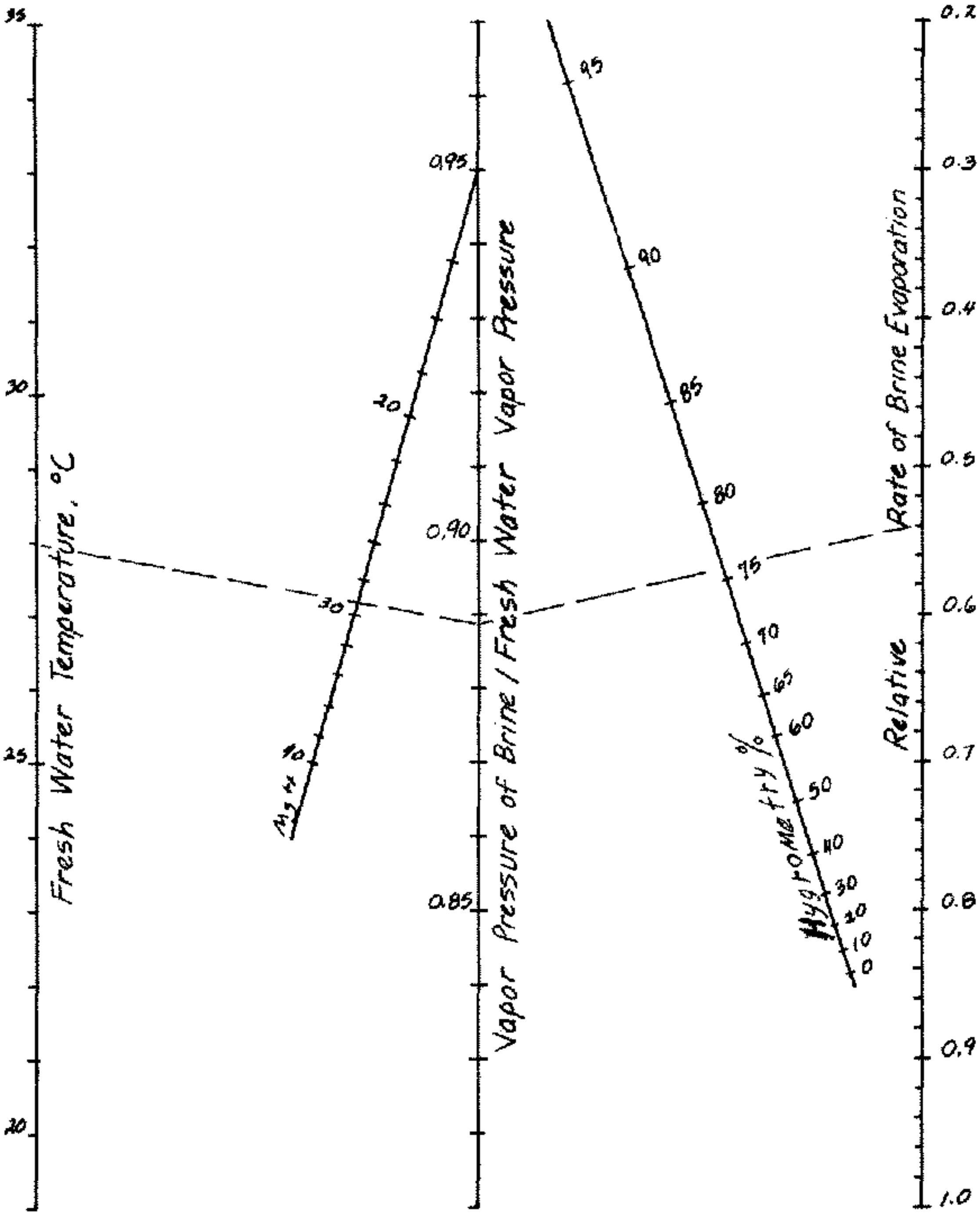

Figure 3. Nomograph to determine evaporation factor between brine and water at various fresh water temperatures, Be' (Mg content) and relative humidity from data by Salin du Midi. (Dale Krrmse Ph.D., P.E., University of Florida).

HYDROBIOLOGY OF SALINAS

In many salinas the microorganism population is out of balance, causing an accumulation of a highly viscous by-product of Coccochloris-organic suspension that seriously suppresses evaporation. By operating the crystallizers in series, the retention time of brine is reduced and consequently lessens the biotic effects on the viscosity. At Araya the operating practice was to operate crystallizers in parallel and discard bittern at 27 Be' because of high viscosity with a recovery of only 50% of the NaCl in the brine fed to crystallizers. A program was recommended to reduce the input of nutrients (from bird droppings) and to increase the biotic consumers of organics. Typically,

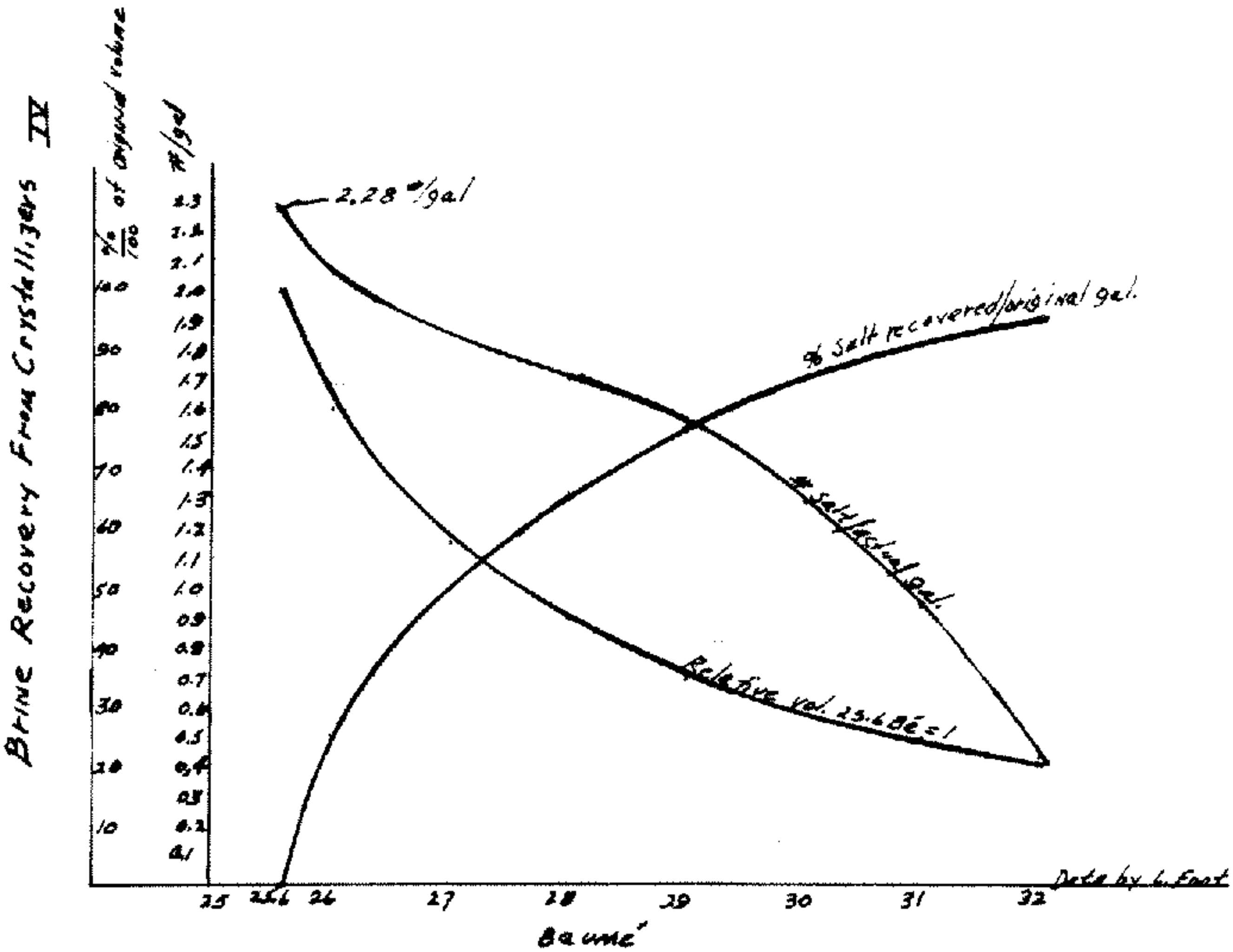

Figure 4. Graph of salt recovery from crystallizers vs Be' of brine being discharged (Cumeragua manual).

these are certain grasses, a limited shell population and *Artemia* (brine shrimp). The biotic population was in balance at Cumeragua, Venezuela and the problem of viscous brine did not exist. The subject of the hydrobiology of solar ponds and control has been well documented in recent years.

SEEPAGE

New salinas historically have seepage problems of varying 'degress that have been corrected by adding trace amounts of fertilizer for one to two years to enhance the growth of algae. The light transmission of pond brine is reduced to 55–70% as measured by a light spectrometer. Colloidal algal particles plug voids in sandy silty soils and also deposit a rubbery algal blanket on the pond bottom. (Figure 6 demonstrates reduction of percolation of various soils before and after depositing an algal blanket).

ALGAL SPLIT

Where rainfall does not permit the maintenance of a silt base over the crystallizer, a proven technique to prevent silt (as it collects) from adhering to the crystallizer floor is to create an algal slime on top of the crystallizer bottom. This mimimizes accumulation of rock and dirt from the crystallizer. The procedure is to fill crystallizers after harvest with 10 to 12 inches of 10–12 Be' brine, and while filling add diammonium phosphate at the rate of about 0.7 ppm to the brine. During the rainy season a slime of algae is grown. When the rainy season is over this brine is returned to the salina and crystallizers are changed with the usual saturated brine. This procedure has the added advantage, when used in new crystallizers, reduce fill voids and percolation.

Crystallizers once having a salt crust rarely have a seepage problem.

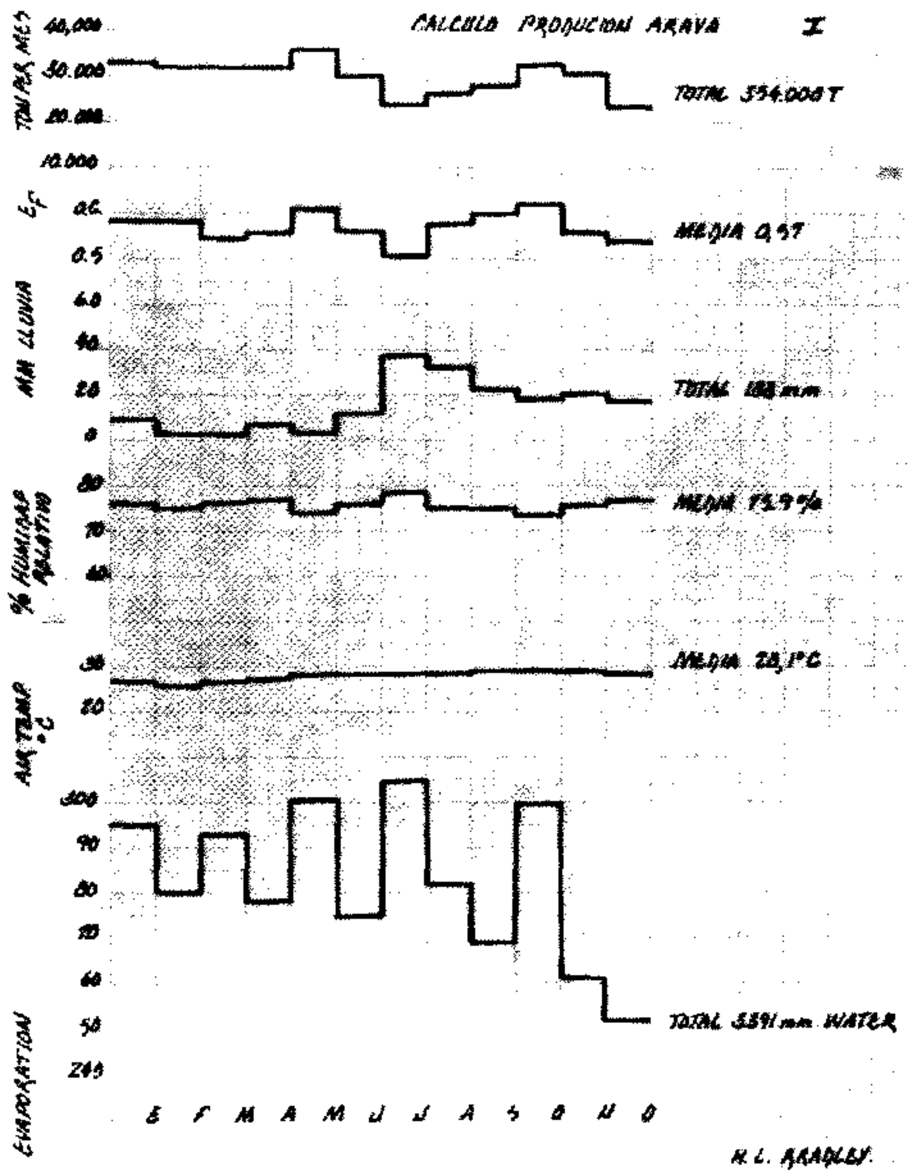

Figure 5. Recapitulation of weather data at Araya, Venezuela and calculated salt production monthly (Bradley).

AUTHORS' COMMENTS

The scope of this paper does not include the theory of solar salt crystallization and its relation to impurities trapped on surfaces and within individual crystalls nor the degree to which impurities are possible to remove in a wash plant (Figure 7). The authors, however, would like to strongly recommend careful study of the paper presented by Masuzawa at the 5th Salt Symposium (1979) and the practical use of his findings for crystallizer and wash plant operation. Breaking up salt clusters in a wash plant is essential to expose impurities to achieve optimum quality.

It was once believed that the cumbersome, costly, high maintenance equipment such as Aikens washers, drag washers, etc., were effective. A much more effective and simple, less costly system of washing consists of using an open impellar pump to break up salt clusters, a hydrocyclone to remove gypsum and silt particles, and a woven wire mesh conveyor to remove Mg^{++} and to dewater. In developing countries having high fuel costs, limited capi-

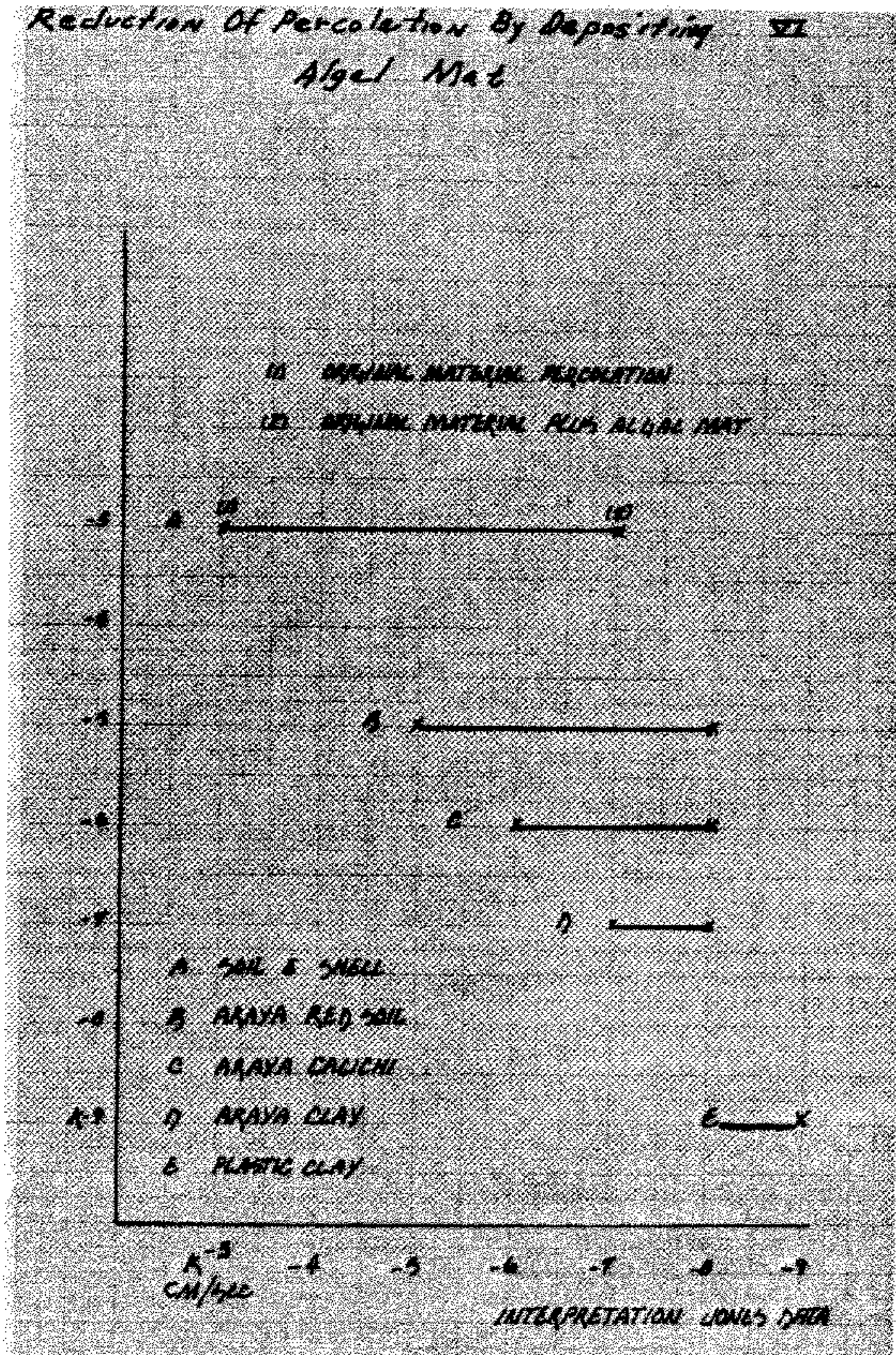

Figure 6. Reduction of percolation by depositing algal mat (data by Jones-Australia).

Figure 7. Photomicrograph of hopper salt crystals (Dow Chemical).

tal and technical personnal, a low cost and simple method is being developed to purify solar salt into table and food consumption products without the necessity of dissolving salt to form a brine, and vacuum evaporating, drying, etc.

ACKNOWLEDGMENT

Acknowledgment is given to Dale Krmse, Ph.D., P.E. of Chemical Engineering Dept., University of Florida, for preparation of the Nomograph III to calculate evaporation factor. His technical interests are in Design & Analysis of Energy Systems and Computer Aided Design & Control. Current research is in process engineering of biomass to methane conversion operations.

REFERENCES

Barr, David J. 1972. The Application of Remote Sensing Techniques to Environmental Problems in the Mineral Industries, Preprint 72-I-321, SME-AIME; October 18–20, 1972.

Bhatt, R. B. 1975. Manufacture of common salt by series feeding system. Salt Research and Industry, vol. 11, no. 7, pp. 9–12.

Block, M. R. et al. 1951. Solar evaporation of salt brines. Industrial & Engineering Chemistry, vol. 43, vo. 7, pp. 1544–53.

Bonython, C. W. 1974. Factors determining the rate of solar evaporation in the production of salt. World Salt Symposium 32, pp. 152–167.

Bradley, H. L. 1981. Maniobra Salmuera y Salina Cumeragua 1/15/81.

Davis, J. S. 1974. Importance of microorganisms in solar salt. World Salt Symposium, 4th, vol. 2.

Davis, J. S. 1978. Biological communities of a nutrient enriched salina. Aq. Bul. 4:23, 42.

Ferguson, J. 1952. The rate of natural evaporation from shallow ponds. Australian Journal of Scientific Research, Series A, vol. 5, pp. 315–330.

de Flers, P. 1969. Solar salt production. World Salt Symposium, pp. 51–61.

de Flers, P. 1969. A new process for washing of solar salt. World Salt Symposium.

Free, K. W. 1958. The production of solar salt. Transactions Instn. Chem. Eng., vol. 36, pp. 115–122.

Garrett, D. E. 1969. Factors in the design of solar salt plants. Part II. Optimum operation of solar ponds. World Salt Symposium, pp. 176–187.

Gallone, P. 1974. Extraction of sodium chloride from sea water. Translation of Ullmann Encyclopadie der technischen Chem., 4th Edition, pp. 1–20.

Garrett, D. E. 1969. Factors in the design of solar salt plants. Part II. Optimum operation of solar ponds and Part I. Pond layout and construction. World Salt Symposium, pp. 168–175.

Harbeck, G. E. 1955. The effect of salinity on evaporation. Geological Survey Professional Paper 272-A, pp. 1–6.

Harbeck, G. E. 1962. A practical field technique for measuring reservoir evaporation utilizing mass-transfer theory. U.S. Geological Professional Papers, pp. 101–105.

Hughes, G. H. 1967. Analysis of techniques used to measure evaporation from Salton sea, Calif. Geological Survey Professional Paper 272-H, pp. 151–176.

Jones, A. G., et al. 1969. Biotechnology solar salt field. pp. 1–16.

Kallerud, M. J. 1969. Advances in solar salt-solar evaporation in multicomponent process. World Salt Symposium, pp. 41–46.

Kaufmann, Dale. 1960. Sodium Chlorida Am. Chem. Soc. Monograph 145, p. 743.

Kohler, M. A. 1952. Lake and pan evaporation (Lake Hefner). Geological Survey Professional Paper 269, pp. 127–157.

Masuzawa, T. 1979. Impurities contained inside the crystals of solar and vacuum evaporated salts. World Salt Symposium, pp. 463–473.

McArthur, J. N. 1979. An approach to process and quality control relevant to solar salt field operations in the northwest of western Australia. World Salt Symposium, pp. 326–334.

Meyers, D. M. and C. W. Boynthon. 1958. The theory of recovering salt from seawater by solar evaporation. Journal Appl. Chem. v. 8, pp. 207–219.

Penmann, H. L. 1948. Natural evaporation from open water, bare soil and grass. Proc. Royal Soc. vol. 193(A), 120–145.

Rands, D. G. 1979. The effect of magnesium on the solar evaporation process. World Salt Symposium, pp. 359-363.

Rohwer, C. 1933. Evaporation from salt solutions and from oil covered water surfaces. Journal of Ag. Research U.S.A., vol. 46, pp. 715–729.

Rothbaum, H. P. 1958. Vapor pressure of sea water concentrates. Chemical & Engineering Chemistry, vol. 3, no. 1, pp. 50-52.

Schneider, J. and H. A. Munter. 1979. Salt works—Natural laboratories for microbiology and geochemical investigations during evaporation of sea water. World Salt Symposium, pp. 1-20.

Sutton, O. G. 1934. Wind structure and Evaporation in a turbulent atmosphere. Proc. Royal Society, pp. 701–722.

Sutton, W. G. 1943. On the equation of diffusion in a turbulent media. Proc. Royal Society.

Union Salinera de Espana. 1979. Memoria. Ensal.

Ver Planck, W. E. 1957. Salt in California. State of Calif. Div. Natural Resources Bulletin 175, pp. 1–168.